PAPER

NJC
www.rsc.org/njc

Synthesis and photochromism of two new 1,2-bis(thiazolyl) perfluorocyclopentenes with chelating sites

Marion Giraud,[a] Anne Léaustic,[a] Marie-France Charlot,[a] Pei Yu,*[a] Michèle Césario,[b] Christian Philouze,[c] Robert Pansu,[d] Keitaro Nakatani[d] and Eléna Ishow[d]

[a] *Laboratoire de Chimie Inorganique (CNRS UMR 8613), Institut de Chimie Moléculaire et des Matériaux d'Orsay, Université Paris XI, Bât. 420, 91405 Orsay cedex, France. E-mail: yupei@icmo.u-psud.fr; Fax: +33 1 69 15 47 54; Tel: +33 1 69 15 61 83*
[b] *Laboratoire de Cristallochimie, Institut de Chimie des Substances Naturelles (CNRS UPR 2301), 91198 Gif-sur-Yvette, France*
[c] *Laboratoire d'Etudes Dynamiques et Structurales de la Sélectivité (CNRS UMR 5616), 38041 Grenoble, France*
[d] *Laboratoire de Photophysique et Photochimie Supramoléculaires et Macromoléculaires (CNRS UMR 8531), ENS Cachan, 61 avenue du Président Wilson, 94235 Cachan cedex, France*

Received (in Toulouse, France) 17th June 2004, Accepted 16th November 2004
First published as an Advance Article on the web 21st January 2005

Two new dithiazolylethenes, **1a** {1,2-bis[5′-methyl-2′-(2″-pyridyl)thiazolyl]perfluorocyclopentene} and **2a** {1,2-bis[4′-methyl-2′-(2″-pyridyl)thiazolyl]perfluorocyclopentene}, have been synthesized. Their photochromic behavior has been fully investigated in solution as well as in the crystalline phase. They display both fatigue-resistant and thermally irreversible photochromic reactions, with more than 80% of the closed-ring forms (**1b** and **2b**, respectively) in the photo-stationary state. Upon UV irradiation, a colorless solution of **1a** turns purple while the yellow color of a **2a** solution becomes more intense. Such marked differences in their electronic absorption spectra are reproduced by DFT calculations. Finally, although structurally closely related, only **1a** shows photochromism in the crystalline phase whereas **2a** displays reversible photo-modulation of fluorescence in solution.

DOI: 10.1039/b409274k

Introduction

Photochromic systems have been attracting much attention for their potential applications in opto-electronic devices.[1] Among various families of organic photochromes, dithienylethenes derivatives are considered to be the most promising photochromic candidates for the development of optical memory and optical switching devices because they usually undergo thermally irreversible and fatigue-resistant photocyclizations between their colorless open-ring and colored closed-ring forms, as shown in Scheme 1.[2]

Besides the color change, photo-switching of the structure between the two forms can also be exploited to reversibly control a wide range of properties that include luminescence,[3–6] refractive index,[7–10] liquid crystal phase,[11–13] redox,[14–15] NLO,[15] acidity,[16] viscosity,[17] charge separation,[18] electron transfer[19] and magnetic couplings,[20] among others. On the other hand, metal ion complexes incorporating photo-switchable di(heteroaryl)ethene units are of particular interest because they would allow investigations of the influence of metal ions on the organic photochromism and may eventually provide a convenient way to control metal-ion-centered properties by the photonic mode. Several examples of such associations have been reported and the photo-modulation of different metal-centered properties have been achieved.[21–27] To date, most of these studies are limited to thienyl and benzothienyl containing ethene derivatives, and only few investigations are devoted to other di(heteroaryl)ethenes as they usually undergo thermally reversible photoreactions.[28–29] It was only recently that the first dithiazolylethene molecules with photochromic features comparable to those of dithienylethenes have been reported.[30–31]

The primary aim of this work was to prepare new photochromic di(heteroaryl)ethenes capable of complexing different metal ions for the design of novel coordination systems with potentially different photo-switchable behavior. Toward this end we have chosen two structurally closely related dithiazolylethene derivatives (Scheme 2) as target molecules.

This choice was motivated by several reasons. First, 2-(2-thiazolyl)pyridine derivatives are known to behave as chelating ligands toward metal ions.[32] Moreover, by offering two different chelating sites (N–N or N–S), they might selectively coordinate different metal ions. Secondly, substitution of the

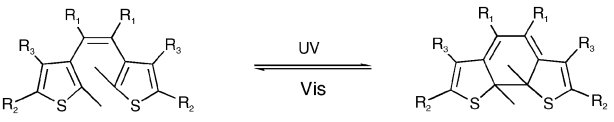

Scheme 1 Photocyclization reaction of diarylethenes.

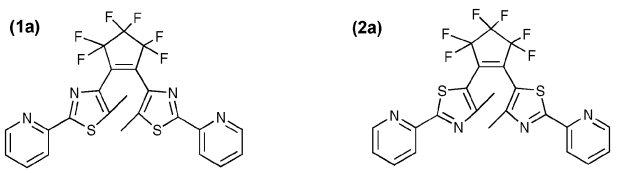

Scheme 2 1,2-Bis[5′-methyl-2′-(2″-pyridyl)thiazolyl]perfluorocyclopentene (**1a**) and 1,2-bis[4′-methyl-2′-(2″-pyridyl)thiazolyl]perfluorocyclopentene (**2a**).

2-pyridyl group for the phenyl one should not alter the main photochromic features of the phenyl-substituted dithiazolylethenes, which are known to display remarkable photochromic behavior such as high thermal stability of both isomers and high fatigue resistance.[31a] Finally, as the two potential chelating sites are relatively close to each other, stronger interactions might be expected between the metals ions. In this paper we report on the syntheses of **1a** and **2a**, their crystal structures, photochromic behavior in solution together with DFT calculations on the origin of the striking differences of the electronic absorption spectra between the two chemical isomers. Crystalline state photochromism of **1a** and photo-modulation of the fluorescent properties of **2a** in solution were also investigated.

Experimental

General

^{1}H NMR spectra were recorded at 200 MHz or 250 MHz (Brüker AC 200 or AM 250), ^{19}F NMR at 235 MHz (Brüker AC 250) in $CDCl_3$ at room temperature. UV-Vis spectra were recorded on a Varian Cary 5E. The fluorescence spectra were recorded on a Spex–Fluorolog spectrometer from Jobin Yvon/Horriba company. Elemental analyses were performed at the Service de Microanalyse, ICSN-CNRS, Gif-sur-Yvette, France.

Reagents and chemicals were used as supplied (Acros, Lancaster or Aldrich) unless otherwise stated. Column chromatography was performed on silica gel (SDS 60) and aluminium oxide (Merck 90). Pyridine-2-thiocarboxamide, 2-bromopropanal dimethyl acetal and 2-(2′-pyridyl)-4-methylthiazole were prepared according to literature methods.[33,34] Special thanks to Prof. M. Irie and Zeon Corporation (Japan) for providing us with the octafluorocyclopentene.

Computational details

DFT calculations were carried out using Becke's three-parameter hybrid functional[35] and the correlation functional of Lee, Yang and Parr (B3LYP),[36] as implemented in the GAUSSIAN98 program.[37] The valence double-zeta basis set (SV) of Ahlrichs *et al.*[38] has been employed for all atoms. As crystallographic data are only available for the open forms of these molecules, the geometries of the four structures were optimized, except for the C–H and C–F distances, which were fixed to their values in the X-ray structure of **1a**. The energies of the excited states and transition oscillator strengths f were calculated by the time dependent DFT formalism (TDDFT)[39] as implemented in the GAUSSIAN98 program. The theoretical electronic spectra were then simulated convoluting each transition with a Gaussian function for the bandwidth at half-height of 2800 cm^{-1} (a value which gives usually molar extinction coefficients of the same order of magnitude as the experimental ones) and area under the curve proportional to f; all these features were then summed up.

Syntheses

2-(2′-Pyridyl)-5-methylthiazole. A solution of 5.52 g (40 mmol) of pyridine-2-thiocarboxamide and 9.15 g (50 mmol) of 2-bromopropanal dimethyl acetal in acetic acid (40 ml) was brought to 100 °C and kept at that temperature overnight under stirring. After removal of acetic acid and addition of 100 ml of H_2O, the pH of the mixture was adjusted to *ca.* 8 with solid Na_2CO_3 and the mixture was then extracted twice with 100 ml of Et_2O. The brown Et_2O phase was decolored with activated carbon and dried over Na_2SO_4. Removal of Et_2O left a brownish solid (5.6 g, 79% yield based on pyridine-2-thiocarboxamide), which was pure enough to use in subsequent reactions. Short column chromatography (silica gel, $CHCl_3$ to 5–10% EtOAc) afforded a pure analytical sample of 2-pyridyl-5-methylthiazole as a yellowish microcrystalline solid. ^{1}H NMR ($CDCl_3$): δ = 2.54 (s, 3H), 7.29 (t, J = 6 Hz, 1H), 7.57 (s, 1H), 7.78 (td, J_1 = 8 Hz, J_1 = 2 Hz, 1H), 8.13 (d, J = 8 Hz, 1H), 8.59 (d, J = 6 Hz, 1H); anal. calcd (%) for $C_9H_8N_2S$ (176.2): C 61.34, H 4.58, N 15.90; found: C 61.11, H 4.64, N 15.89.

2-(2′-Pyridyl)-4-methylthiazole. 2-(2′-Pyridyl)-4-methylthiazole · HCl was prepared as described in the literature.[40] Neutralization in H_2O gave the title compound as an almost colorless microcrystalline solid with an overall yield of 72%.

2-(2′-Pyridyl)-4-bromo-5-methylthiazole. To a solution of 2.11 g (12 mmol) of 2-(2′-pyridyl)-5-methylthiazole in 25 ml of $CHCl_3$ and 25 ml of MeCN was slowly added 1.25 ml (24 mmol) of Br_2. After refluxing for 48 h the solvents were removed under vacuum. H_2O (100 ml) and CH_2Cl_2 (50 ml) were added to the solid residue and the pH of the aqueous phase was adjusted to *ca.* 8 with solid Na_2CO_3. The aqueous phase was washed once again with 50 ml of CH_2Cl_2. The combined organic phase was washed with brine and dried over Na_2SO_4. After removal of CH_2Cl_2, column chromatography (silica gel, CH_2Cl_2) of the solid residue afforded 1.92 g of the title compound as a colorless microcrystalline solid with 62% yield. ^{1}H NMR ($CDCl_3$): δ = 2.47 (s, 3H), 7.32 (m, 1H), 7.78 (m, 1H), 8.14 (d, J = 8 Hz, 1H), 8.58 (d, J = 4 Hz, 1H); anal. calcd (%) for $C_9H_7BrN_2S$ (255.1): C 42.37, H 2.77, N 10.98; found: C 42.25, H 2.80, N 10.92.

2-(2′-Pyridyl)-5-bromo-4-methylthiazole. The compound was synthesized in a similar manner as 2-(2′-pyridyl)-5-bromo-4-methylthiazole except the refluxing time was reduced to *ca.* 6 h and Et_2O was used for the extraction. After column chromatography (silica gel, CH_2Cl_2 to 5% Et_2O), the title compound was obtained as a colorless microcrystalline solid with *ca.* 90% yield. ^{1}H NMR ($CDCl_3$): δ = 2.48 (s, 3H), 7.32 (t, J = 6 Hz, 1H), 7.79 (m, 1H), 8.10 (d, J = 8 Hz, 1H), 8.58 (d, J = 4 Hz, 1H); anal. calcd (%) for $C_9H_7BrN_2S$ (255.1): C 42.37, H 2.77, N 10.98; found: C 42.21, H 2.83, N 10.77.

1,2-Bis[5′-methyl-2′-(2″-pyridyl)thiazolyl]perfluorocyclopentene (1a). 2-(2-Pyridyl)-4-bromo-5-methylthiazole (1.02 g, 4 mmol) was dissolved under argon in *ca.* 60 ml of Et_2O distilled from sodium and benzophenone. The solution was cooled to −78 °C with partial reprecipitation of the starting compound. nBuLi (1.8 ml, 4.5 mmol) in hexane (2.5 M) was slowly added to the mixture over *ca.* 15 min. After stirring for 30 min at the same temperature, *ca.* 0.27 ml (2 mmol) of octafluorocyclopentene (by means of a pre-cooled syringe) was quickly added into the red-brown mixture. The stirring was continued for *ca.* 2 h at the same temperature and then allowed to slowly warm up to room temperature and stirred overnight. An aqueous solution (20 ml) containing 1 ml of concentrated aqueous HCl was added to the brown-colored solution with some suspension. After *ca.* 30 min of stirring the pH of the aqueous phase was brought to *ca.* 8 with solid $NaHCO_3$. The Et_2O phase was separated, washed with H_2O (60 ml) and dried over Na_2SO_4. After removal of Et_2O the residue was column chromatographed using first neutral Al_2O_3 (Et_2O–hexane 2 : 3) and then silica gel (Et_2O—CH_2Cl_2, 5%). Finally, the photochromic **1a** was recrystallized in hexane to afford **1a** as colorless microcrystals (0.40 g 38% yield). M.p. 143 °C (uncorrected); ^{1}H NMR ($CDCl_3$): δ = 2.09 (s, 6H), 7.31 (m, 2H), 7.47 (m, 2H), 8.13 (d, J = 8 Hz, 2H), 8.56 (d, J = 4 Hz, 2H); ^{19}F NMR [$CDCl_3$, (trifluoromethyl)benzene as external reference]: δ = −5.46 (q, ^3J = 5.5 Hz, 2F), 16.06 (t, ^3J = 5.5 Hz, 4F); anal. calcd (%) for $C_{23}H_{14}F_6N_4S_2$ (524.5): C 52.67, H 2.69, N 10.68; found: C 53.11, H 2.82, N 10.69. Single crystals of **1a** suitable

for X-ray analysis were obtained by slow evaporation of a hexane solution.

1b. ^{1}H NMR ($CDCl_3$): δ = 2.10 (s, 6H), 7.50 (m, 2H), 7.89 (m, 2H), 8.34 (d, J = 8 Hz, 2H), 8.73 (d, J = 5 Hz, 2H); ^{19}F NMR ($CDCl_3$): δ = −6.93 (m, 2F), 11.60 (d, J_{AB} = 275 Hz, 2F), 14.76 (d, J_{AB} = 275 Hz, 2F).

1,2-Bis[4′-methyl-2′-(2″-pyridyl)thiazolyl]perfluorocyclopentene (2a). **2a** was prepared in a similar way to **1a**: 1.8 ml (4.5 mmol) of nBuLi in hexane (2.5 M) was slowly added to an Et_2O solution (*ca.* 60 ml) containing 1.02 g (4 mmol) of 2-(2-pyridyl)-5-bromo-4-methylthiazole at −78 °C. After 10–15 min of stirring, 0.27 ml (2 mmol) of octafluorocyclopentene was quickly syringed into the mixture. The stirring was continued for *ca.* 1 h at the same temperature and then allowed to slowly warm up to room temperature and stirred overnight. To the orange solution was added with stirring an aqueous solution (20 ml) containing 1 ml of concentrated HCl. After *ca.* 15 min the pH of the aqueous phase was adjusted to *ca.* 8. The Et_2O phase was collected, washed with H_2O (*ca.* 60 ml) and dried with Na_2SO_4. After removal of Et_2O the orange oil was column chromatographed (silica gel, CH_2Cl_2 to 10% Et_2O in CH_2Cl_2). Evaporation of the yellow fractions containing **2a** left a yellow oil that, after being triturated with *ca.* 20 ml of hexane and allowed to stand overnight, gave **2a** as a yellow microcrystalline solid (0.65 g, 62% yield). M.p. 160 °C (uncorrected); ^{1}H NMR ($CDCl_3$): δ = 2.09 (s, 6H), 7.36 (m, 2H), 7.77 (m, 2H), 8.11 (d, J = 8 Hz, 2H), 8.58 (d, J = 5 Hz, 2H); ^{19}F NMR ($CDCl_3$): δ = −4.42 (q, ^3J = 5.5 Hz, 2F), 17.10 (t, ^3J = 5.5 Hz, 4F); anal. calcd (%) for $C_{23}H_{14}F_6N_4S_2$ (524.5): C 52.67, H 2.69, N 10.68; found: C 52.85, H 2.73, N 10.56. Single crystals of **2a** suitable for X-ray analysis were obtained by slow evaporation of a diethyl ether solution.

2b. ^{1}H NMR ($CDCl_3$): δ = 1.57 (s, 6H), 7.49 (m, 2H), 7.88 (m, 2H), 8.32 (d, J = 7 Hz, 2H), 8.73 (d, J = 5 Hz, 2H); ^{19}F NMR ($CDCl_3$): δ = −7.53 (m, 2F), 7.34 (d, J_{AB} = 270 Hz, 2F), 12.06 (d, J_{AB} = 270 Hz, 2F).

Crystal structure determination†

1a. A crystal of 0.35 × 0.40 × 0. 60 mm^3 was mounted on an Enraf-Nonius Kappa-CCD diffractometer. A full sphere of data was collected by ϕ axis rotation with an increment of 2° over 360° and 20 s exposure per degree. Denzingering was accomplished by measuring each frame twice. Data were analyzed using Kappa-CCD software.[41] Cell dimensions were refined with HKL-Scalepack.[42] and data reduction performed with Denzo.[42] The structure was solved by direct methods (SHELXS-86)[43] and was refined on F^2 for all reflections by least-squares methods using SHELXL-93.[44] The asymmetric unit consists of one molecule of the photochromic compound. All hydrogen atoms were located by difference Fourier syntheses. They were modeled at their theoretical positions using an isotropic thermal factor equal to 1.2 times that of the bonded atom and introduced in the refinement cycles. The five-membered fluoro ring is affected by disorder. Two positions were found in the difference Fourier syntheses. Better convergence was obtained with occupancies of 0.80 and 0.20 for the flip-flop motion of the C7A–C6A–C6B–C7B plane. Refinement was pursued with restraints and the minor position was refined isotropically. The final conventional R is 0.0496 for 4078 $F_o > 4\sigma(F_o)$, 352 parameters and 46 restraints, and 0.0749 for all data, wR (F^2) = 0.17 for all reflections, $w = 1/[\sigma^2 (F_o)^2 + (0.1028\,P)^2 + 1.07\,P]$ where $P = (F_o^2 + 2F_c^2)/3$. The largest difference peak and hole are 0.3 and −0.2 e Å^{-3}.

† CCDC reference numbers 235922 and 231160 for **1a** and **2a**, respectively. See http://www.rsc.org/suppdata/nj/b4/b409274k/ for crystallographic data in .cif or other electronic format.

2a. The *Pbcn* orthorhombic yellow-green prism (~0.20 × 0.20 × 0.18 mm^3) of the compound was obtained by evaporation at room temperature of a diethyl ether solution. The crystal was stuck on a glass fiber and centered on the goniometer of a Nonius (Bruker) CAD-4 diffractometer. Unit cell parameters were obtained by least squares refinement with CAD-4 software[45] of 25 reflections that had been automatically centered on the diffractometer. The crystal decayed by 4.64% over the time of the data collection. Intensity data were collected with the CAD-4 software and were processed using the TeXsan program package.[46] The structure was solved by direct methods with the use of the SIR92 software[47] and refined using TeXsan. The extinction was refined. The final refinement involved an anisotropic model for all non-hydrogen atoms. The hydrogen atoms were set geometrically or using the difference Fourier. They were recalculated before the last refinement cycle. The model displays half a molecule of the compound in the asymmetric unit. The whole molecule is generated by symmetry expansion.

Quantum yield determination

Solutions of **1** and **2** were irradiated by a 450 W mercury lamp (Oriel) through narrow band interference filters of appropriate wavelength. During irradiation, the absorption change was monitored *in situ* by a CCD camera mounted with a spectrometer (Princeton Instruments). The irradiation flux was measured by a power meter (Ophir). Data were analyzed by a method adapted from a previously described one.[48] Irradiation of **1a** and **2a** in the UV allowed us to determine $\Phi_{a\rightarrow b}$ and irradiation of photo-stationary mixtures in the visible allowed us to determine $\Phi_{b\rightarrow a}$.

Results and discussion

Syntheses

Both **1a** and **2a** were prepared in three steps as shown in Scheme 3: (1) pyridinethiazoles were obtained by reactions of pyridine-2-thiocarboxamide[33] with, respectively, 2-bromopropanal dimethyl acetal[34] in acetic acid or 1-chloro-2-propanone in ethanol by the Hantzsch method; (2) bromination of the thiazole rings was carried out with bromine in a mixture of chloroform and acetonitrile; (3) bromine-lithium exchange followed by nucleophilic displacement of fluoride of octafluorocyclopentene gave **1a** and **2a**. All new compounds were characterized by ^{1}H NMR and elementary analysis. Single crystals of **1a** and **2a** suitable for crystal structure determinations were obtained by slow evaporation at room temperature of a hexane solution of **1a** and a diethyl ether solution of **2a**.

Solution photochromic behavior

Fig. 1 shows the absorption spectral changes of **1a** and **2a** in MeCN at room temperature upon UV irradiation (reagent grade MeCN was used without prior drying and degassing). The initial solution of **1a** was colorless with an intense absorption band in the UV region (λ_{max} 310 nm). Upon UV irradia-

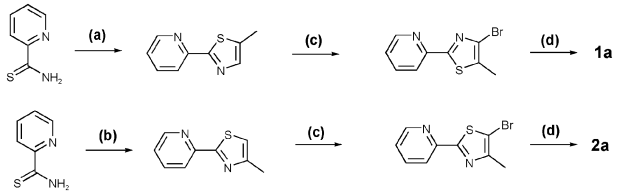

Scheme 3 Syntheses of **1a** and **2a**. (a) $CH_3CHBrCH(OCH_3)_2$ in acetic acid, 100 °C; (b) $ClCH_2COCH_3$ in EtOH, reflux; (c) Br_2 (2 equiv.) in $CHCl_3$–MeCN (50 : 50), reflux; (d) (1) nBuLi (1.1 equiv.) in Et_2O, −78 °C; (2) C_5F_8 (0.5 equiv.).

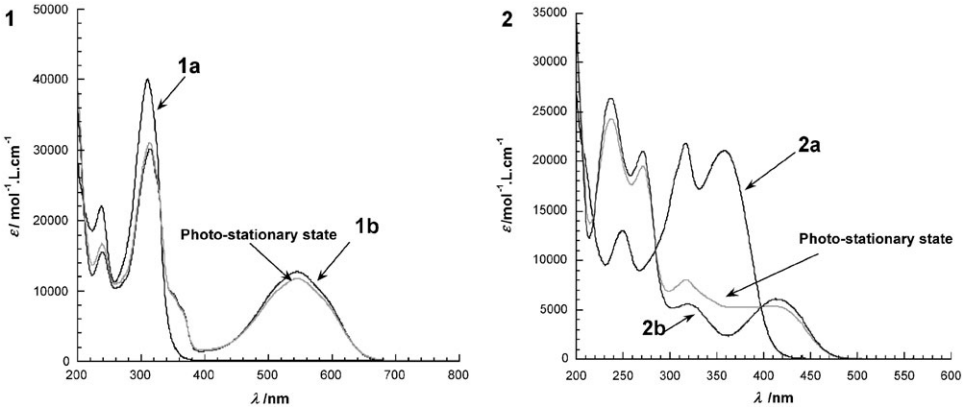

Fig. 1 UV-visible absorption spectra of the open form **a**, closed form **b** and photo-stationary states of **1** (left) and **2** (right).

tion (320 nm) the solution turned red-violet with concomitant decrease of the band in the UV and appearance of a new broad band in the visible (λ_{max} 545 nm).

Monitoring of the reaction by ^{1}H NMR (in CD_3CN or $CDCl_3$) showed clearly that the color change corresponds to the transformation of the open-ring form **1a** into that of closed-ring form **1b**. The red-violet color was easily bleached with visible light irradiation (550 nm) with the initial spectrum being fully recovered.

The situation was much different for **2a**. The solution of **2a** was pale yellow with several intense bands in the UV (λ_{max} 317, 358 nm). UV irradiation (365 nm) turned the solution to orange with important changes in the UV region and appearance of a new band in the visible (λ_{max} 414 nm), associated to the formation of the closed-ring form **2b**. The initial color and spectrum were easily restored by visible light irradiation (450 nm). For both molecules, such a coloring and bleaching cycle could be repeated many times without any sign of spectral changes, suggesting their good fatigue-resistance characteristics, probably similar to those of the corresponding di(phenylthiazolyl)perfluorocyclopentenes previously reported.[31a] It is worth noting that both in the open and closed forms the molar extinction coefficients of the lowest energy bands of **1** and **2** are nearly in a 2 to 1 ratio.

The fractions of **1b** and **2b** in the photo-stationary state were estimated to be respectively 0.90 and 0.80 on the basis of ^{1}H NMR, and they were further confirmed by comparing their photo-stationary state spectra with those of pure **1b** and **2b** (Fig. 1), which were isolated by column chromatography in the dark (silica gel, CH_2Cl_2) and characterized by ^{1}H NMR and ^{19}F NMR. It is worth noting that the monitoring of photoreactions is greatly simplified by use of ^{19}F NMR due to much larger differences between the spectra of the two isomers (see Experimental).

The quantum yields of cyclization ($\Phi_{a\rightarrow b}$) and ring-opening reactions ($\Phi_{b\rightarrow a}$) at room temperature were measured by irradiating MeCN solutions of **1** and **2** with a mercury lamp through band pass filters (see Experimental for details). The results are given in Table 1, along with the main UV-Vis data of both isomers of **1** and **2**. For comparison, we have also included reported data (in hexane) for the corresponding phenyl-substituted dithiazolylethenes, that is, 1,2-bis[5′-methyl-2′-phenylthiazolyl]perfluorocyclopentene (noted as **3**) and 1,2-bis[4′-methyl-2′-phenylthiazolyl]perfluorocyclopentene (noted as **4**).[31a] As it can be seen from Table 1, the solution behavior of **1** and **2** is similar to that of the corresponding **3** and **4**, except that the measured quantum yield of the ring-opening reaction for **2b** is much higher than that reported for **4b**. The fact that the measurements were not made in the same solvent (MeCN for **1** and **2**, hexane for **3** and **4**) may, at least partly, account for such a difference in the quantum yield. The striking differences between **1** and **2** in the electronic absorption spectra can be attributed, as for **3** and **4**, to the difference of π conjugation length in the different isomers.[31a] In order to have a better understanding on how the electronic absorption spectra of **1** and **2** depend on the way the thiazole group is connected to the perfluorocyclopentene ring, DFT calculations were performed on both isomers of the two photochromes.

Computational study

DFT calculations using a valence double-zeta basis set were performed on both the open-ring and closed-ring forms of the two photochromes. As crystallographic data are available only for the open-ring forms, DFT geometry optimizations were carried out for the four isomeric structures of **1** and **2** with only the C–H and C–F distances kept frozen to their values in the X-ray structure of **1a**. This simplification has been made to decrease the optimization computation time and did not affect the skeleton of the molecules. It is worth noticing that the calculated structure of **1a** is less symmetric with more geometric differences between the two side arms than that of **2a**. Photochromic properties involve electronic transitions of lower energy (visible and near-UV regions); so we focus the study on this part of the spectra that involves the frontier orbitals. The HOMOs and LUMOs are reported in Fig. 2 for the two open-ring forms and in Fig. 3 for the two closed-ring forms. In both the open-ring and the closed-ring forms these orbitals are

Table 1 Absorption maxima, molar extinction coefficients of open and closed ring forms, quantum yields of cyclization and ring-opening reactions for **1** and **2** as well as those reported for **3** and **4**[a,b]

	λ_{max}/nm (ε_{max}/M^{-1}cm^{-1})	$\Phi_{a\rightarrow b}$ (λ_{irr}/nm)		λ_{max}/nm (ε_{max}/M^{-1}cm^{-1})	$\Phi_{b\rightarrow a}$ (λ_{irr}/nm)
1a[c]	310 (40 000)	0.17 ± 0.01 (313)	**1b**[c]	545 (12 700)	0.035 ± 0.005 (547)
2a[c]	358 (21 000)	0.50 ± 0.01 (365)	**2b**[c]	414 (6000)	0.52 ± 0.02 (436)
3a[d]	300 (34 000)	0.32 (313)	**3b**[d]	525 (10 000)	0.02 (492)
4a[d]	363 (21 000)	0.22 (366)	**4b**[d]	406 (7000)	0.01 (420)

[a] λ_{max} and λ_{irr} stand respectively for the maximum absorption wavelength and the irradiation wavelength. [b] It has to be stated that even though no significant solvatochromic effects have been noticed for **1** and **2** when passing from hexane to acetonitrile, the quantum yield may be affected by the solvent used. [c] In MeCN. [d] In hexane.

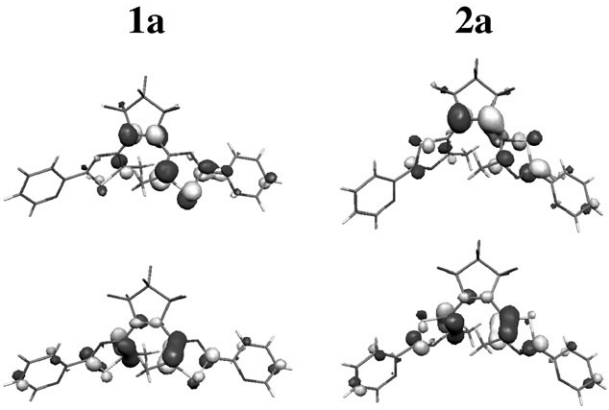

Fig. 2 HOMO (bottom) and LUMO (top) of the open forms **1a** (left) and **2a** (right).

located on the six carbon atoms of the hexatriene (open) or cyclohexadiene (closed) framework, that is in the part that undergoes the major changes in the cyclization process. These orbitals are, as expected, strikingly reminiscent of the HOMO and LUMO of hexatriene (**a** form) or cyclohexadiene (**b** form) (Fig. 4).

In the open forms, the HOMOs consist of π bonds essentially located between the two pairs of thiazolyl carbons C1═C2 and C5═C6 and to some extent between the carbons C3 and C4 of cyclopentene. They are very similar in the two isomers **1a** and **2a**, with almost identical contributions from the sulfur atoms and the pyridine rings and have nearly the same energy. The LUMOs of these open forms, both characterized mainly by the pronounced π antibonding contribution between C3 and C4, differ, however, in a significant way. There is no π contribution from carbon atoms C2 and C5 of the hexatriene in **1a**, while the LUMO of **2a** possesses significant π C2═C3 and C4═C5 connections. Hence, the LUMO of **2a** is lower in energy than that of **1a** and consequently the calculated HOMO–LUMO energy gap δ is about 34 200 cm^{-1} in **1a** as compared to 28 500 cm^{-1} in **2a**. We have to mention that in the LUMO of **1a** the electronic density extends to only one pyridine group through a π bonding C(thiazoyle)═C(pyridine) connection. This small dissymmetry of the two side arms results in orbitals LUMO + 1 and LUMO + 2 close in energy to the LUMO. Consequently, these orbitals will also give significant contributions to the low-energy part of the spectrum. This does not occur for the more symmetric **2a** form since the first vacant orbitals are well-separated in energy.

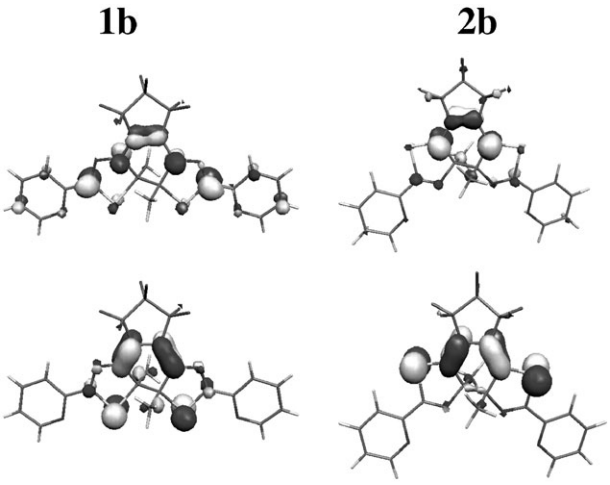

Fig. 3 HOMO (bottom) and LUMO (top) of the closed forms **1b** (left) and **2b** (right).

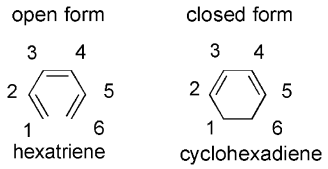

Fig. 4 Atom labeling for hexatriene and cyclohexadiene.

The frontier orbitals of the closed forms recall those of the butadiene fragment of the cyclohexadiene core, but the calculations show that the orbitals extend more into the arms in **1b** than in **2b**. Indeed, the electronic density in the HOMOs is located in the π bonding C2═C3 and C4═C5 and in the sulfur lone pairs in **2b**; in **1b** this orbital delocalizes over the thiazole rings, decreasing consequently the stabilization due to this bonding effect. In the LUMOs, the two antibonding contributions between C2–C3 and C4–C5 prevail over the effect of the π bonding between C3 and C4. The resulting increase of energy is then smaller in the more extended LUMO of **1b** than in the in-core localized orbital of **2b**. It is interesting to notice that in the closed forms the extension of the electronic density over more atoms produces opposite effects on the HOMO and LUMO energies. The final result is a smaller energy gap δ in **1b** (~19 800 cm^{-1}) than in **2b** (~28 100 cm^{-1}).

Fig. 5 shows the calculated electronic spectra of the two forms of **1** obtained by the procedure described in the Experimental. The first three excited states of **1a**, obtained essentially by mono-excitations from HOMO to LUMO, HOMO to LUMO + 1 and HOMO to LUMO + 2 in order of increasing energy, have close excitation energies due to the orbital pattern discussed before. As a result, the three transitions from the ground state to these excited states are almost degenerate and are together responsible for the 'calculated band' with an absorption maximum at *ca.* 314 nm. For the closed-ring form **1b** the band calculated in the visible region at 605 nm corresponds to a single transition with mainly HOMO to LUMO character.

For compound **2**, the lowest energy bands have calculated λ_{max} at ~406 nm for the open form and ~423 nm for the closed form. They both result from a single transition, which is essentially a HOMO to LUMO mono-excitation. Hence, the wavelength shifts between **1a** and **2a** or between **1b** and **2b** reflect the differences in the corresponding HOMO–LUMO energy gaps.

In the open-ring forms as well as in the closed-ring forms the ratios of the calculated intensities for the two isomers agree rather well with the experimental data: the 'bands' involved in the photochromic process are almost half less intense in **2** than

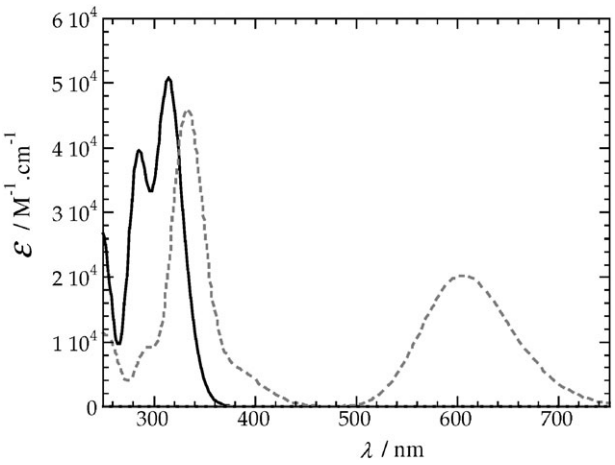

Fig. 5 Calculated electronic absorption spectra of **1a** (—) and **1b** (- - -).

in **1** for both forms. As explained before, for the open forms several transitions contribute to the low energy band in **1** but only one in **2**. For the closed forms, the more localized character of the HOMO and LUMO in **2b** as compared to **1b** is responsible for the lower transition dipole moment, consequently leading to less intense transitions for **2b** than for **1b**. In conclusion, although DFT calculations are performed on isolated molecules with a single optimized geometry and they neglect vibrational effects, the calculations reproduce rather well the general shapes of the experimental spectra as well as the energies and intensities of the low-energy bands. Indeed, it is remarkable to notice that the maximum difference in energy between the simulated and experimental values does not exceed 10%.

Thermal stability

The thermal stability of the close-ring forms **1b** and **2b** was measured at 80 °C in mesitylene (1,3,5-trimethylbenzene). A solution of **1a** (or **2a**) was UV irradiated and its UV-Vis spectrum recorded at room temperature. The solution was then left in the dark at 80 °C for 48 h before the recording of a new UV-Vis spectrum. For both molecules **1** and **2**, there were no detectable absorption spectral changes even after 48 h at 80 °C. This result is in agreement with the fact that the thiazole group is known to have, like thiophene, a low aromatic stabilization energy so that a large thermal stability is predicted by theory for diarylethenes with such aryl groups.[30,31]

Fluorescent properties of 2

It is worth noting that **2a** is fluorescent in solution as well as in the crystalline phase while **1a** does not possess this property. The fluorescence spectral changes of a **2a** solution under UV excitation are shown in Fig. 6.

With UV excitation at λ_{ex} = 352 nm, a broad emission band centered around 500 nm was observed. The excitation spectrum (not shown) confirmed that the emissive species was indeed **2a**. Moreover, the intensity of this emission band decreased quickly with further UV irradiation and dropped to about one-third of the initial value in the photo-stationary state. Visible light (450 nm) irradiation restored the initial capability of the solution to fluoresce. Such reversible fluorescence changes, already observed for other diarylethenes, are clearly due to the photochromic reaction that, in the present case, reversibly transforms the fluorescent open-ring form **2a** to the non-fluorescent closed-ring form **2b**. The fluorescence quantum yield (Φ_f) of **2a** was measured in MeCN (quinine sulfate in H_2O as reference). The low value obtained (Φ_f = 5‰) can probably be ascribed, at least partly, to the high quantum yield of photocyclization measured for **2a**. The fact that in the crystalline state **2a** was found to be highly fluorescent with an emission profile similar to that in solution also supports this idea since the competitive photochromic reaction, operative in solution, is not observed in the crystalline phase.

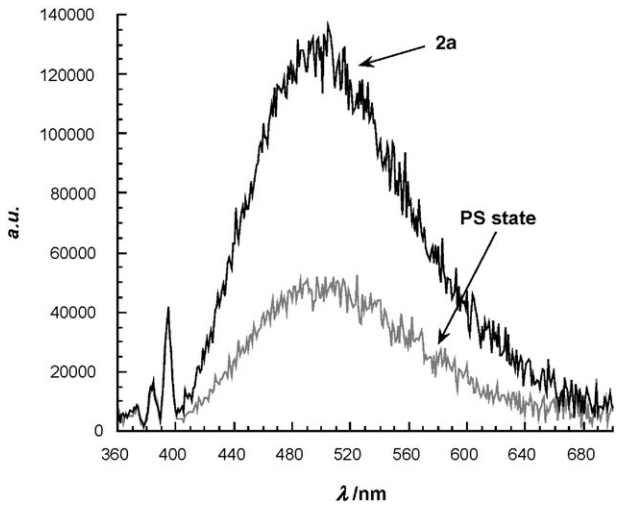

Fig. 6 Fluorescence emission spectra of **2a** and its photo-stationary (PS) state at λ_{ex} = 352 nm.

Photochromism in the crystalline phase and crystal structures of 1a and 2a

Some diarylethenes with thiophene or benzothiophene as aryl groups are known to show crystalline phase photochromism. Various potential applications in photonic devices have been proposed for such photochromic crystals.[49] During our investigations only **1a** was found to display photochromism in the crystalline phase, as shown in Fig. 7. Upon UV irradiation (365 nm), the colorless single crystal of **1a** turned dark violet. This violet color remained stable in the dark, but could be easily bleached by visible light irradiation (550 nm). This coloring and bleaching cycle could be performed several times but a prolonged irradiation alters the quality of the crystal and eventually breaks it up. In order to understand the difference of behavior between the two compounds, their crystal structures were determined. The main X-ray crystallographic data are summarized in Table 2.

The molecular structures of both **1a** and **2a** (Fig. 8) are characterized by two common features: (1) near planarity between the pyridine and thiazole groups on each side arm of the photochromes **1a** and **2a**; (2) the two methyl groups attached to the photo-reactive carbon atoms in both molecules are in the trans conformation and the distance between the two reactive carbon atoms is 3.71 Å for **1a** and 3.56 Å for **2a**.

For the photochromic reaction to take place in the crystalline phase it is usually believed that two conditions in the molecular structure have to be met: (1) the two R substituents on the photo-reactive carbon atoms must be in trans conformation because only the antiparallel conformer is photoactive in the conrotatory cyclization; (2) the two reactive carbon atoms should be close enough to allow the photoreaction

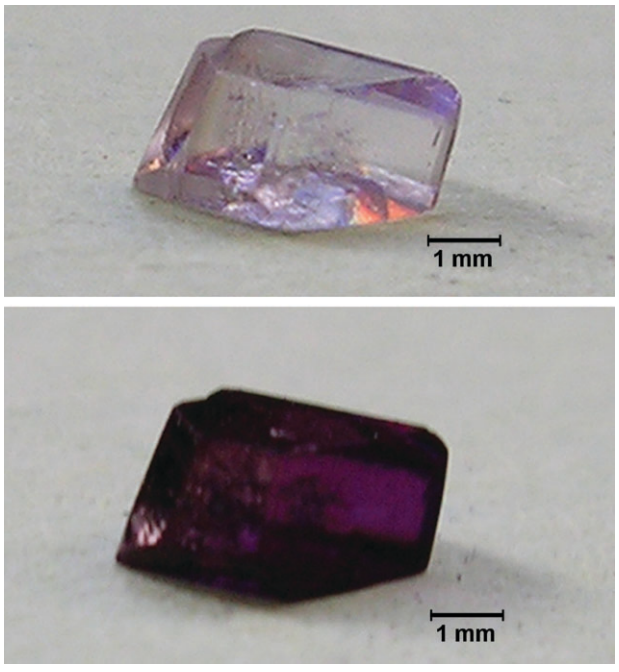

Fig. 7 Photographs of a single crystal of **1a** before (top) and after (bottom) irradiation at 365 nm.

Table 2 Crystallographic data of **1a** and **2a**

	1a	**2a**
Empirical formula	$C_{23}H_{14}F_6N_4S_2$	$C_{11.5}H_7F_3N_2S$
Formula weight	524.50	262.25
T/K	293	293
Wavelength/Å	0.710 73	1.541 78
Crystal system	Monoclinic	Orthorhombic
Space group	$P21/n$	$Pbcn$
a/Å	16.492(6)	10.902(1)
b/Å	8.379(3)	12.360(1)
c/Å	16.790(7)	17.546(2)
α/°	90	90
β/°	93.52(4)	90
γ/°	90	90
Volume/Å^3	2316(2)	2364
Z	4	8
Reflections collected	10909	10046
Independent reflections	5694	2434
R(int)	0.0229	0.0847
Observed reflections	4078	2056
R_1 [$I > 2\sigma(I)$]	0.0496	0.0673
wR_2 [$I > 2\sigma(I)$]	0.1401	0.1183
R_1 (all data)	0.0749	0.0848
wR_2 (all data[a])	0.1698	0.1333

[a] The number of data are 5694 and 2434 for **1a** and **2a**, respectively.

and this distance is typically shorter than 4.2 Å.[50] However, the correlation between structure and photoreactivity in the crystalline phase seems more complex since **2a** is not found to display (under the experimental conditions) such a behavior while its molecular structure fulfils the above criteria. To our knowledge, similar observations have been made for several other diarylethene derivatives.[51,52] One of the possible reasons for the difference is that one has to consider not only the molecular structure but also the crystal packing. The comparison of the two crystal structures reveals stronger intermolecular interactions in **2a** than in **1a**. First, relatively strong π stackings (average distance of 3.6 Å) exist between the thiazole ring of one molecule and the pyridine ring of adjacent molecules for **2a**; whereas in **1a** no such close contacts can be found. Moreover, the fact that the thiazole ring is involved in the π stacking may considerably restrict its rotation, necessary for the electrocyclization.

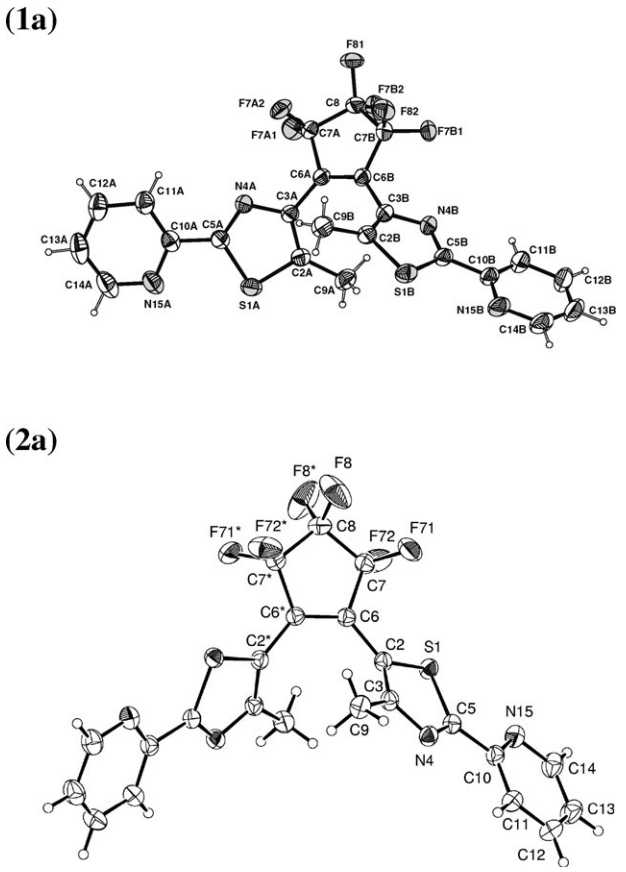

Fig. 8 ORTEP views of **1a** (top, complete atom labeling) and **2a** (bottom, partial atom labeling for the part of the molecule generated by symmetry), showing 25% displacement ellipsoids.

Conclusion

Two new dithiazolylethenes with the potential ability to chelate different metal ions have been synthesized and fully characterized. Both molecules **1a** and **2a** display fatigue-resistant and thermally irreversible photochromic reactions in solution. The marked differences in their electronic absorption spectra results from the way the thiazole is connected to the central perfluorocyclopentene ring, which is in accordance with DFT calculations. Furthermore, interesting crystalline phase photochromism is observed for **1a**, which is, as far as we know, the first thiazole-based diarylethene with such a property, while **2a** shows reversible photo-modulation of fluorescence in solution. We are currently investigating interactions between such dithiazolylethenes and different metals ions in order to design new photochromic complexes with different photoswitchable behaviors.

References

1 (*a*) J. C. Crano and R. J. Guglielmetti, *Organic Photochromic and Thermochromic Compounds*, Plenum, New York, 1999; (*b*) ed. M. Irie, *Chem. Rev.*, 2000, **100**, special issue.
2 M. Irie, *Chem. Rev.*, 2000, **100**, 1685.
3 G. M. Tsivgoulis and J. M. Lehn, *Angew. Chem., Int. Ed. Engl.*, 1995, **34**, 1119.
4 (*a*) M. Takeshita and M. Irie, *Chem. Lett.*, 1998, 1123; (*b*) M.-S. Kim, T. Kawai and M. Irie, *Chem. Lett.*, 2001, 702; (*c*) T. Kawai, T. Sasaki and M. Irie, *Chem. Commun*, 2001, 711; (*d*) A. Osuka, D. Fujikane, H. Shinmori, S. Kobatake and M. Irie, *J. Org. Chem.*, 2001, **66**, 3913; (*e*) K. Yagi, C. F. Soong and M. Irie, *J. Org. Chem.*, 2001, **66**, 5419; (*f*) K. Yagi and M. Irie, *Bull. Chem. Soc. Jpn.*, 2003, **76**, 1625; (*g*) T. Fukaminato, T. Kawai, S. Kobatake and M. Irie, *J. Phys. Chem. B*, 2003, **107**, 8372.
5 J. Ern, A. T. Bens, H.-D. Martin, S. Mukamel, S. Tretiak, K. Tsyganenko, K. Kuldova, H. P. Trommsdorff and C. Kryschi, *J. Phys. Chem. A*, 2001, **105**, 1741.
6 T. B. Norsten and N. R. Branda, *J. Am. Chem. Soc.*, 2001, **123**, 1784.
7 (*a*) T. Yoshida, K. Arishima, F. Ebisawa, M. Hoshino, K. Sukegawa, A. Ishikawa, T. Kobayashi, M. Hanazawa and Y. Horikawa, *J. Photochem. Photobiol., A*, 1996, **95**, 265; (*b*) M. Hoshino, F. Ebisawa, T. Yoshida and K. Sukegawa, *J. Photochem. Photobiol., A*, 1997, **105**, 75.
8 J. Biteau, F. Chaput, K. Lahlil and J. P. Boilot, *Chem. Mater.*, 1998, **10**, 1945.
9 M.-S. Kim, H. Maruyama, T. Kawai and M. Irie, *Chem. Mater.*, 2003, **15**, 4539.
10 S. Chen, H. P. Chen, Y. Geng, S. D. Jacobs and K. L. Marshall, *Adv. Mater.*, 2003, **15**, 1061.
11 C. Denekamp and B. L. Feringa, *Adv. Mater.*, 1998, **10**, 1080.
12 (*a*) K. Uchida, Y. Kawai, Y. Shimizu, V. Vill and M. Irie, *Chem. Lett.*, 2000, 654; (*b*) T. Yamaguchi, T. Inagawa, H. Nakazumi, S. Irie and M. Irie, *J. Mater. Chem.*, 2001, **11**, 2453.
13 K. E. Maly, M. D. Wand and R. P. Lemieux, *J. Am. Chem. Soc.*, 2002, **124**, 7898.
14 T. Saika, M. Irie and T. Shimidzu, *Chem. Commun.*, 1994, 2123.
15 S. L. Gilat, S. H. Kawai and J. M. Lehn, *Chem.-Eur. J.*, 1995, **1**, 275.
16 S. H. Kawai, S. L. Gilat and J. M. Lehn, *Eur. J. Org. Chem.*, 1999, 2359.
17 L. N. Lucas, J. V. Esch, R. M. Kellogg and B. L. Feringa, *Chem. Commun.*, 2001, 759.
18 J. M. Endtner, F. Effenberger, A. Hartschuh and H. Port, *J. Am. Chem. Soc.*, 2000, **122**, 3037.

19 P. A. Liddell, G. Kodis, A. L. Moore, T. A. Moore and D. Gust, *J. Am. Chem. Soc*., 2002, **124**, 7668.
20 (*a*) K. Matsuda and M. Irie, *J. Am. Chem. Soc*., 2000, **122**, 7195; (*b*) K. Matsuda and M. Irie, *Chem.-Eur. J*., 2001, **7**, 3466; (*c*) K. Matsuda, M. Matsuo, S. Mizoguti, K. Higashiguchi and M. Irie, *J. Phys. Chem. B*., 2002, **106**, 11218.
21 M. Munakata, L. P. Wu, T. Kuroda-Sowa, M. Maekawa, Y. Suenaga and K. Furuichi, *J. Am. Chem. Soc*., 1996, **118**, 3305.
22 (*a*) A. Fernandez-Acebes and J. M. Lehn, *Adv. Mater*., 1998, **10**, 1519; (*b*) A. Fernandez-Acebes and J. M. Lehn, *Chem.-Eur. J*., 1999, **5**, 3285.
23 S. Fraysse, C. Coudret and J. P. Launay, *Eur. J. Inorg. Chem*., 2000, 1581.
24 (*a*) K. Matsuda, K. Takayama and M. Irie, *Chem. Commun*., 2001, 363; (*b*) K. Yakayama, K. Matsuda and M. Irie, *Chem.-Eur. J*., 2003, **9**, 5605; (*c*) K. Matsuda, K. Takayama and M. Irie, *Inorg. Chem*., 2004, **43**, 482.
25 (*a*) T. B. Norsten and N. R. Branda, *Adv. Mater*., 2001, **13**, 347; (*b*) E. Murguly, T. B. Norsten and N. R. Branda, *Angew. Chem., Int. Ed*., 2001, **40**, 1752.
26 (*a*) B. Chen, M. Wang, Y. Wu and H. Tian, *Chem. Commun*., 2002, 1060; (*b*) H. Tian, B. Chen, H. Tu and K. Müllen, *Adv. Mater*., 2002, **14**, 918.
27 H. Konaka, L. P. Wu, M. Munakata, T. Kuroda-Sowa, M. Maekawa and Y. Suenaga, *Inorg. Chem*., 2003, **42**, 1928.
28 K. Uchida, T. Matsuoka, K. Sayo, M. Iwamoto, S. Hayashi and M. Irie, *Chem. Lett*., 1999, 835.
29 A. Heynderickx, A. M. Kaou, C. Moustrou, A. Samat and R. Guglielmetti, *New J. Chem*., 2003, **27**, 1425.
30 S. Iwata, Y. Ishihara, C. Qian and K. Tanaka, *J. Org. Chem*., 1992, **57**, 3726.
31 (*a*) K. Uchida, T. Ishihawa, M. Takeshita and M. Irie, *Tetrahedron*, 1998, **54**, 6627; (*b*) S. Takami, T. Kawai and M. Irie, *Eur. J. Org. Chem*., 2002, 3796.
32 A. T. Baker, H. A. Goodwin and A. D. Rae, *Inorg. Chem*., 1987, **26**, 3513.
33 E. C. Taylor and J. A. Zoltewicz, *J. Am. Chem. Soc*., 1960, **82**, 2656.
34 F. Bellesia, M. Boni, F. Ghelfi and U. M. Pagnoni, *Gazz. Chim. Ital*., 1993, **123**, 629.
35 A. D. Becke, *J. Chem. Phys*., 1993, **98**, 5648.
36 C. Lee, W. Yang and R. G. Parr, *Phys. Rev. B*, 1988, **37**, 785.
37 M. J. Frisch, G. W. Trucks, H. B. Schlegel, G. E. Scuseria, M. A. Robb, J. R. Cheeseman, V. G. Zakrzewski, J. A. Montgomery, Jr., R. E. Stratmann, J. C. Burant, S. Dapprich, J. M. Millam, A. D. Daniels, K. N. Kudin, M. C. Strain, O. Farkas, J. Tomasi, V. Barone, M. Cossi, R. Cammi, B. Mennucci, C. Pomelli, C. Adamo, S. Clifford, J. Ochterski, G. A. Petersson, P. Y. Ayala, Q. Cui, K. Morokuma, D. K. Malick, A. D. Rabuck, K. Raghavachari, J. B. Foresman, J. Cioslowski, J. V. Ortiz, A. G. Baboul, B. B. Stefanov, G. Liu, A. Liashenko, P. Piskorz, I. Komaromi, R. Gomperts, R. L. Martin, D. J. Fox, T. Keith, M. A. Al-Laham, C. Y. Peng, A. Nanayakkara, C. Gonzalez, M. Challacombe, P. M. W. Gill, B. G. Johnson, W. Chen, M. W. Wong, J. L. Andres, M. Head-Gordon, E. S. Replogle and J. A. Pople, *GAUSSIAN 98 (Revision A.6)*, Gaussian, Inc., Pittsburgh, PA, 1998.
38 A. Schaefer, H. Horn and R. Ahlrichs, *J. Chem. Phys*., 1992, **97**, 2571.
39 M. E. Casida, C. Jamorski, K. C. Casida and D. R. Salahub, *J. Chem. Phys*., 1998, **108**, 4439.
40 P. Karrer and J. Schukri, *Helv. Chim. Acta*, 1945, **28**, 820.
41 *Kappa-CCD Software*, Enraf-Nonius, Delft, The Netherlands, 1997.
42 Z. Otwinovski and W. Minor, *Methods Enzymol*., 1997, **276**, 307.
43 G. M. Sheldrick, *Acta Crystallogr., Sect A*, 1990, **46**, 467.
44 G. M. Sheldrick, *Program for the Refinement of Crystal Structures*, University of Göttingen, Göttingen, Germany, 1993.
45 *CAD-4 Software*, Enraf-Nonius, Delft, The Netherlands, 1989.
46 *TeXsan. (version 1.7.)*, Molecular Structure Corporation, The Woodlands, TX, USA, 1992-1997.
47 A. Altomare, G. Cascarano, C. Giacovazzo and A. Guagliardi, *J. Appl. Crystallogr*., 1993, **26**, 343.
48 H. Rau, G. Greiner, G. Gauglitz and H. Meier, *J. Phys. Chem*, 1990, **94**, 6523.
49 M. Irie, S. Kobatake and M. Horichi, *Science*, 2001, **291**, 1769.
50 S. Kobatake, K. Uchida, E. Tsuchida and M. Irie, *Chem. Commun*., 2002, 2804.
51 F. Sun, F. Zhang, H. Guo, X. Zhou, R. Wang and F. Zhao, *Tetrahedron*, 2003, **59**, 7615.
52 K. Morimitsu, S. Kobatake and M. Irie, *Tetrahedron Lett*., 2004, **45**, 1155.